

This manuscript is a non-peer-reviewed pre-print submitted to EarthArXiv. This manuscript has been submitted for publication in *Water Resources Research* and is currently under review.

## **Data from the drain: a sensor framework that captures multiple drivers of chronic floods**

**Adam Gold<sup>1</sup>, Katherine Anarde<sup>2</sup>, Lauren Grimley<sup>3</sup>, Ryan Neve<sup>4</sup>, Emma Rudy Srebnik<sup>5</sup>, Thomas Thelen<sup>2</sup>, Anthony Whipple<sup>4</sup>, Miyuki Hino<sup>5,6</sup>**

<sup>1</sup>University of North Carolina at Chapel Hill Institute for the Environment, Chapel Hill, NC

<sup>2</sup>North Carolina State University, Department of Civil, Construction, and Environmental Engineering, Raleigh, NC

<sup>3</sup>University of North Carolina at Chapel Hill, Department of Earth, Marine and Environmental Sciences, Chapel Hill, NC

<sup>4</sup>University of North Carolina at Chapel Hill Institute of Marine Sciences, Morehead City, NC

<sup>5</sup>University of North Carolina at Chapel Hill, Environment, Ecology, and Energy program, Chapel Hill, NC

<sup>6</sup>University of North Carolina at Chapel Hill, Department of City and Regional Planning and Environment, Chapel Hill, NC

Corresponding author: Adam Gold (Email: [gold@unc.edu](mailto:gold@unc.edu), Twitter: [@acgold](https://twitter.com/acgold))

**Contributions** (using the CRediT taxonomy - <https://casrai.org/credit/>)

**Adam Gold** - formal analysis; data curation; visualization; writing-original draft; software; methodology

**Katherine Anarde** - writing-original draft; investigation; funding acquisition; project administration; conceptualization

**Lauren Grimley** - resources; writing-original draft; investigation

**Ryan Neve** - methodology; investigation; software; writing-original draft; validation

**Emma Rudy Srebnik** - resources; writing-review and editing

**Thomas Thelen** - resources; writing-original draft; investigation;

**Anthony Whipple** - methodology; investigation; software; writing-original draft; validation

**Miyuki Hino** - writing-original draft; investigation; funding acquisition; project administration; conceptualization

### **Key Points:**

- We present a new low-cost, open-source sensor framework that measures coastal flooding from multiple sources
- For a five month deployment, 25% of floods were driven by land-based sources and not predicted by tide gauge proxies
- Measures of flood frequency based on tide gauge records are likely underestimates where stormwater networks are routinely impaired

### **Abstract**

Tide gauge records are commonly used as proxies to detect coastal floods and project future flood frequencies. While these proxies clearly show that sea-level rise will increase the frequency of coastal flooding, tide gauges do not account for land-based sources of coastal flooding and therefore likely underestimate the current and future frequency of coastal flooding. Here we present a new sensor framework for measuring the incidence of coastal floods that captures subterranean and land-based contributions to flooding. The low-cost, open-source sensor framework consists of a storm drain water level sensor, roadway camera, and wireless gateway that transmit data in real-time. During five months of deployment in the Town of Beaufort, North Carolina, 24 flood events were recorded. 25% of those events were driven by land-based sources – rainfall, combined with moderate high tides and reduced capacity in storm drains – and would not have been detected using tide gauge proxies. This finding suggests that tide-gauge proxies likely underestimate flood frequency in areas where the stormwater networks are at a reduced drainage capacity due to inundation by receiving waters. Our results highlight the benefits of capturing multiple drivers of coastal flooding by instrumenting stormwater networks directly. More accurate estimates of the frequency and drivers of floods in low-lying coastal communities can enable the development of more effective long-term adaptation strategies.

## 1 Introduction

Coastal communities around the world are confronting the growing challenge of sea-level rise (SLR). In the United States, six feet of SLR by 2100 could affect 1.7 million homes and up to 3.6 million people (Bernstein et al., 2019; Hauer et al., 2016). Already, coastal communities from Florida to Alaska are actively investing in reducing their risk from SLR, whether through a full community relocation or large-scale infrastructure investments (Bronen & Chapin, 2013; Gornitz et al., 2020; Molinaroli et al., 2019). Long before communities are permanently inundated, they experience recurrent flooding (Dahl et al., 2017). As local SLR, land subsidence, and heavy rainfall events increase, so does the frequency of flooding in low-lying coastal areas (Sweet et al., 2018). The tidal cycle now takes place on higher average sea levels, resulting in “sunny-day” flooding of roadways during high tides. Because sea water infiltrates drainage systems at even low tidal levels (Gold, Brown, et al., 2022), ordinary rain storms can now cause flash floods. We refer to locations that experience flooding multiple times per year, from drivers other than extreme storms (e.g., tropical cyclones, nor’easters), as chronically flooded.

It is well-established that higher sea levels will lead to more frequent flooding, but it is not clear which areas will be affected, how quickly, and how intensely. Chronic coastal flooding is difficult to monitor because the floods are hyper-local, creating a patchwork of affected intersections, blocks, or homes, and because floods can be caused by multiple sources. While chronic flooding is often associated with tidally-driven sunny-day flooding, it can also be influenced by groundwater, wind, rainfall runoff, and riverine discharge (Loftis et al., 2018; Moftakhari et al., 2017). The role of stormwater drainage systems is also poorly understood. In Norfolk, VA, recent instrumentation efforts have shown that SLR has reduced the city’s stormwater system capacity by 50% (independent of the tide), and thus is hampering the ability of the system to handle heavy rainfalls (Coutu, 2021). The viability of stormwater systems is also affected by rising groundwater, which has led to corrosion and failure of underground infrastructure in Hawaii and Florida (Befus et al., 2020; Habel et al., 2020), a problem that is likely to occur elsewhere. These subterranean components of flooding are not typically included in large-scale SLR driven flood risk assessments (e.g., “bathtub” inundation modeling approaches, Sweet et al., 2018) or smaller-scale assessments of compound coastal floods (Jane et al., 2020).

While local residents often know of problem areas to avoid, information on the drivers, frequency, and spatial extent of these floods is rarely gathered systematically. One commonly-used proxy for coastal flooding is days above a locally-defined water level threshold at tide gauges. For example, the National Oceanic and Atmospheric Administration’s (NOAA) National Ocean Service (NOS) has defined gauge-specific water level thresholds that they refer to as high-tide flooding (HTF) thresholds, though the selected water level is not based on impacts to land. Based on those thresholds, 12 tide gauges set records for flood frequency (i.e., days with water levels exceeding the HTF threshold) in 2018, and nationally, flood frequency is expected to double or triple by 2030 (Sweet et al., 2020). Tide gauge-based proxies clearly show the implications of rising sea levels, but they likely paint an incomplete picture. First, the U.S. tide gauge network is sparse, and water levels can vary substantially over small geographies due to different winds, bathymetry, proximity to rivers or inlets, and other characteristics. Tide gauges also only show contributions to flooding within large water bodies (tides, surge, river discharge), and they will miss events that occur due to a combination of land-based sources (rainfall runoff, groundwater, infrastructure). Moore & Obradovich (2020) found that local tweets about flooding increased well before tide gauge water levels surpassed the National Weather Service thresholds

in several major cities. This suggests flooding may be occurring more often than existing flood proxies indicate.

There have been several recent efforts to develop instrumentation for measuring chronic floods, the majority of which rely on ultrasonic depth sensors (i.e., air sonars). The FloodSense sensor is open-source and uses downward-looking ultrasonic sensors to detect street flooding by attaching the sensors to subaerial structures (e.g., street signs); the data are communicated in real-time using long-range radio (LoRa; FloodNet, 2022). Because the sensor is deployed subaerially, it cannot capture subterranean impairments to stormwater networks that may contribute to street floods. The StormSensor, which also relies on an ultrasonic depth sensor, is proprietary and is designed to be deployed within storm drains while still communicating data at regular intervals using LoRa. Notably, a nonprofit spent \$280,000 USD to collect data on stormwater capacity in Norfolk using 25 of the StormSensors in 2021 (Coutu, 2021). In addition to the high cost, upon submergence, the StormSensors (and all ultrasonic depth sensors) cannot provide information about street water levels or flood extent. Pressure transducers are commonly used to measure water depths in water bodies at low-cost (Lyman et al., 2020; Maisano et al., 2019; Temple et al., 2020; Ware & Fuentes, 2018), however, they similarly only provide information about water levels at a single point. If deployed within a storm drain, real-time communication can also be impeded by stormwater infrastructure (grates, pipes). While not necessary for measuring flood incidence, real-time communication ensures no loss of data (e.g., due to sensor damage or theft) and allows data to be used for hazard identification by stakeholders, practitioners, and researchers alike.

Here we present the utility of a new sensor framework for measuring the incidence and drivers of chronic floods. The sensor framework – which we coin SuDS: the **Sunny Day** flood Sensors – consists of a pressure logger deployed within a storm drain and a subaerially-mounted communications gateway equipped with a camera. Data are streamed to a web-based (open-source) platform for real-time communication of chronic flood hazards. This framework overcomes limitations of existing instrumentation by 1) identifying street flooding from a combination of subterranean and subaerial sources, and 2) allowing for real-time communication of flood depths and visual confirmation of flood extent. Further, the sensor framework is open-source and can be manufactured using online tutorials at low-cost. We confirm through a 5-month deployment of the SuDS in Beaufort, North Carolina that land-based sources contribute significantly to chronic coastal floods at this location, and flood frequency is underestimated by the local tide gauge proxies.

## **2 Materials and Methods**

Detailed step-by-step instructions for manufacturing the SuDS framework are available online (Gold, Anarde, et al., 2022). Sensor hardware and software are all open-source. At the time of publication, the SuDS framework costs approximately \$650 USD to manufacture (excluding handheld tools, 3D printers, and soldering irons), which is comparable to the cost of a single commercial (real-time) pressure transducer. Herein we summarize both sensor components – the in situ pressure logger and the subaerial camera and gateway – and the workflow for real-time communication. We then describe the initial SuDS deployment in Beaufort, North Carolina (NC).

## 2.1 Pressure logger in storm drain

We designed a pressure logger that can be deployed in storm drains to measure real-time water levels coming into storm drains from both below (e.g., tides) and above (e.g., rainfall) while transmitting these data to a subaerial communications gateway (Figure 1A). All electronics for the pressure logger are located within a watertight PVC housing attached to the bottom of the grate covering the storm drain. The electronics housing connects to the pressure transducer via a vertical PVC pipe that extends to near the bottom of the drain (Figure 1B). We use a low-cost BlueRobotics pressure transducer that can measure up to 10 m depths with a reported depth resolution of 0.16 mm. The transducer communicates with an open-source data logger (SparkFun OpenLog Artemis) that records absolute pressure and temperature, which is later converted to water depth in the cloud (Section 2.3). The real-time data collected by the data logger are transmitted via Bluetooth to a communication gateway (described below) using a low-energy Bluetooth board. The logger electronics are powered with three D-cell batteries and secured to the PVC electronics housing using custom 3D-printed mounts (Figure 1D). The D-cell batteries in the pressure logger are replaced approximately every 4-6 months.

Pressure is sampled every six minutes, but this rate can be modified to suit local conditions. The data logger and Bluetooth board are powered off between samples to reduce battery consumption. The logger is mounted at an elevation in the storm drain so that the pressure transducer is out of water and able to dry at least once every 24 hours; this is a requirement for proper functionality of the transducer (as prescribed by the manufacturer). When the pressure logger is entirely submerged, the Bluetooth connection with the gateway is lost, and data are stored locally on the data logger. Once the water recedes, the Bluetooth connection is reestablished and the previously logged data are downloaded by the gateway. The pressure transducer is sensitive to temperature. To account for this, we calibrate each transducer in the lab by recording pressure at known depths for a range of temperatures. The results are used to develop a transducer-specific equation that corrects the pressure readings for temperature. Raw pressure readings are corrected for temperature at the communications gateway (Section 2.2) and drift is corrected in the cloud (Section 2.3).

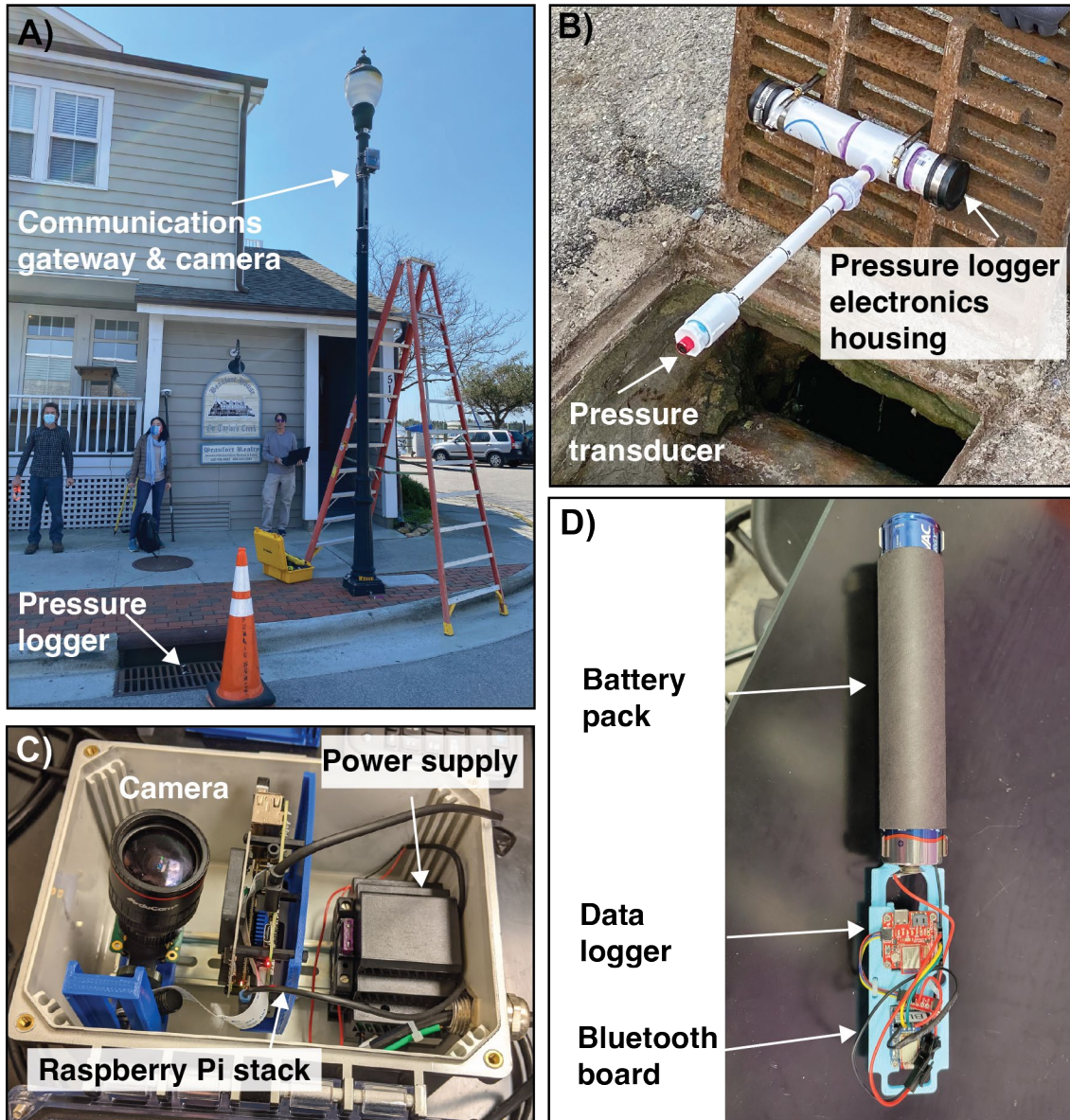


**Figure 1.** (A) Installation of the Sunny Day Flood Sensors (SuDS) in Beaufort, North Carolina. The SuDS consist of (B) a pressure logger deployed within a storm drain and (C) a subaerially-mounted communications gateway equipped with a camera. The gateway is powered by an outlet on the light post. (D) Internal view of the pressure logger. The SuDS are open-source and can be manufactured using online tutorials at low-cost.

## 2.2 Subaerial camera and communications gateway

The camera and communications gateway (collectively referred to as “the gateway” herein) is mounted to a light post within Bluetooth range of the pressure logger (Figure 1A). Although not limited to deployment on light posts, the gateway requires an electrical outlet for power and must be within range of an accessible WiFi signal. The gateway contains a Raspberry Pi 4 Model B Quad Core computer (with Bluetooth and WiFi) running the Linux-based Raspberry Pi OS, an uninterruptible power supply (UPS) module, and an adjustable focal length



camera, all housed in a waterproof, polycarbonate enclosure retrofitted with an optical dome. Heatsinks and a CPU fan prevent gateway components from overheating. All components are secured within the waterproof enclosure using a DIN rail and custom 3D-printed mounts (Figure 1C).

The gateway manages communication between both the pressure logger and cloud data storage. Communication errors from events such as logger submergence and weak signal strength along either link are handled in the following manner. A continuously running Python program manages data flowing both from the pressure logger and to the cloud-based database. Data flow is shown in Figure 2. Upon collecting a sample, data collected on the pressure logger are stored to an internal file and transmitted over Bluetooth to the gateway. Bluetooth is then powered off and the logger enters a deep sleep mode to conserve power until the next sample. The gateway is always watching for the Bluetooth signal to appear. When it does, a connection is established and the gateway waits a predetermined amount of time for data to appear from the pressure logger. If data are not received within the expected time an attempt is made to recover from an error condition. Otherwise, if valid data are received, it is checked to see if it is sequential with previously received data. If so, the record is logged to files on the gateway. If it is not sequential, then the gateway downloads the relevant file(s) from the pressure logger filesystem to catch up. The gateway then attempts to transmit data through a data application programming interface (API) to the cloud (Section 2.3). If the gateway is in “catch-up” mode, the database is polled to find the most recent observation, and data are transmitted using the data cache stored in the gateway filesystem. Since pressure data are stored both on the logger and the gateway, gaps in the data can be recovered automatically despite any communication lapses.

Image acquisition is scheduled by time (every six minutes) using a built-in Linux-based Cron facility. This enables visual confirmation of roadway flooding and provides an indication of flood extents. Images are written to the gateway’s local storage and kept for four weeks. Images are transmitted to cloud storage through a photo API by first polling the database to find the most recent image and continuing from that point.

### 2.3 Data processing and storage in the cloud

The general workflow of data transmission to the cloud is shown in Figure 2. Two application programming interfaces (APIs) are used to route raw data from the gateway to cloud storage. The “photo” API receives images from the Raspberry Pi and saves them to Google Drive. The data API receives raw temperature and pressure data from the Raspberry Pi and stores it in a cloud-hosted PostgreSQL database table. Both APIs were created using the FastAPI framework in Python (<https://fastapi.tiangolo.com>), containerized using Docker (Merkel, 2014), and deployed on RedHat’s OpenShift platform. The APIs offer functions that respond to “POST” and “GET” requests to communicate with the Raspberry Pi and prevent duplicate data transmission (double sided arrows in Figure 3).

Raw pressure and temperature data are post-processed in the cloud. A scheduled processing function runs every 6 minutes and converts the raw absolute pressure data into water depth (above the pressure transducer) using atmospheric pressure data from the closest NOAA tide gauge. Water depth is then assessed for quality control issues (e.g., erroneous jumps in pressure) and converted to drift-correct water levels relative to the road and NAVD88. Drift is common in low-cost pressure transducers (Lyman et al., 2020). Here, we identify and correct for drift by setting the running minimum water depth equal to zero (i.e., when no water is in the storm drain and the pressure transducer is recording atmospheric pressure). The methodology for

drift correction is shown in Figure S1. Notably, although the pressure transducer used in the pressure logger has a manufacturer-reported long-term stability of  $\pm 2$  mbar/yr, during our 5 month deployment, the observed drift was significantly large: equivalent of 0.5 feet of water depth over 5 months.

Once in the cloud, data and images can be loaded to other web interfaces for real-time communication of flood hazards.

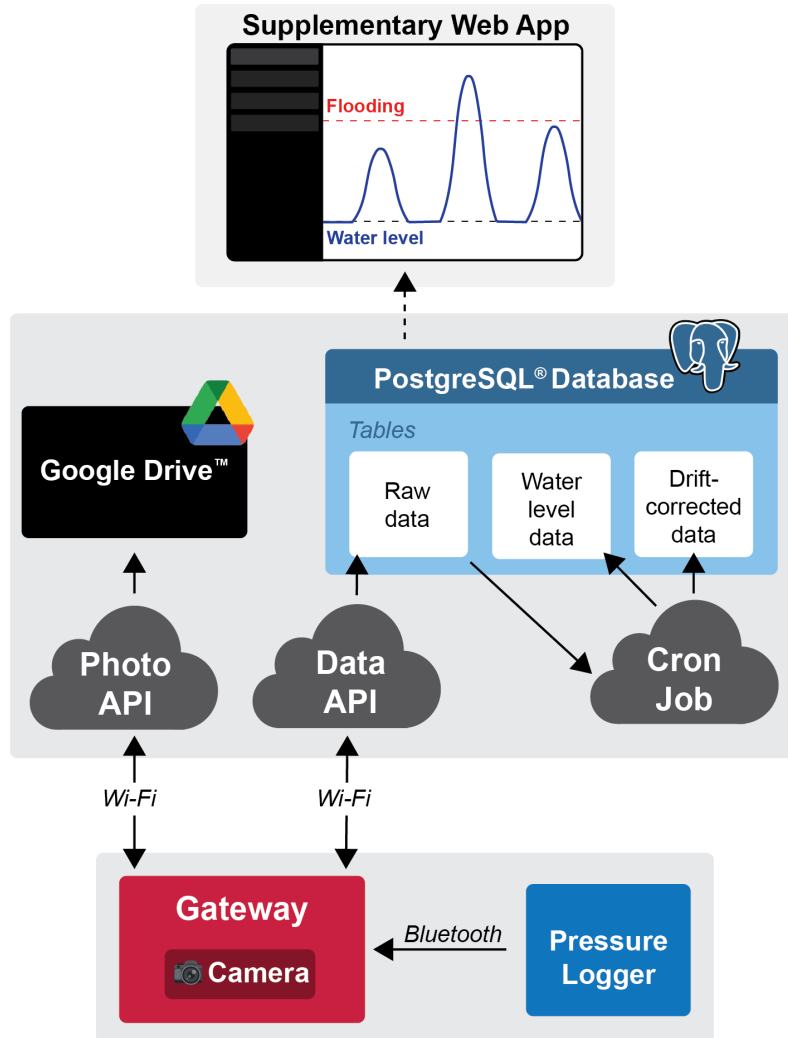


**Figure 2.** Schematic of data transmission to the cloud and post-processing workflow. After data is collected in the field (bottom), application programming interfaces (APIs) are used to transmit data to cloud-based storage and route data through post-processing algorithms. Cloud storage allows data to be easily visualized through supplementary web applications (optional pathway, top).

#### 2.4 Case study location: Beaufort, North Carolina

Our case study location for assessing the utility of this new sensor framework for measuring the incidence and drivers of chronic floods is Beaufort, North Carolina (Figure 3). Beaufort is a historic small town on the southeastern coast of North Carolina and a popular



tourist destination. Downtown Beaufort is a hub of activity during the summer months, but roadway flooding has rendered shops and restaurants inaccessible during high-tide events in recent years. Readings from a local tide gauge (NOAA 8656483) surpassed the National Ocean Service's water-level threshold for "high-tide flooding" on one day in 2000 and four days in 2019, and it is projected to surpass the threshold 6-15 days by 2030 (Sweet et al., 2020).

Working with Beaufort officials, we installed a single SuDS pressure logger and gateway in June 2021 at the location of a flood hotspot on Front Street, the main waterfront roadway in Beaufort (Figure 3B). This portion of Front Street is protected by bulkheads, which according to local officials, are rarely overtopped during high-tide events. Therefore, stormwater infrastructure was hypothesized to play a large role in chronic roadway floods. The stormwater network at this location consists of two storm drains located on opposite sides of the street that connect to an outfall one block to the southeast. This outfall empties into Taylors Creek, a tidal creek connected to the Atlantic Ocean via Beaufort Inlet. The pressure logger was installed in the drain on the south side of the street and the gateway on a neighboring light post (Figure 1A). The pressure transducer was positioned just above the bottom of the storm drain, at the elevation of the bottom of the outfall pipe (3.14 feet below the top of the roadway), such that the transducer records air pressure when the drain is completely empty of water. To visually confirm roadway flooding and capture a larger range of flood extent, we pointed the camera at the storm drain across the street, which is at a slightly lower elevation (Figure 3B). A NOAA tide gauge (8656483) is located 1 km west of the SuDS, which allows for robust comparison of measured flood frequency with those estimated using local tide gauge proxies. Data from a National Weather Service station 2 km north of the SuDS (Beaufort Smith Field, KMRH) was used to analyze precipitation patterns during observed flood events (Figure 3A).

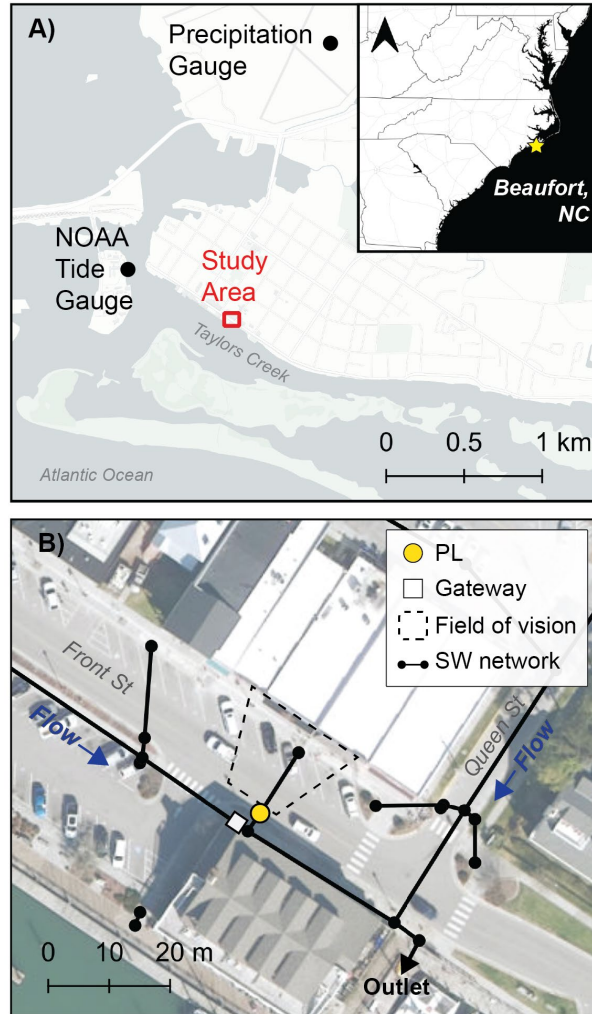


**Figure 3.** **A)** Overview map of Beaufort, NC and the location of a local NOAA tide gauge (8656483). **B)** Map of the study area showing the stormwater (SW) network (and designed flow direction), location of the SuDS pressure logger (PL), gateway, and field of view for the camera.

### 3 Results and Discussion

#### 3.1 Flood measurements

Over the course of five months (June 22, 2021 to November 30, 2021), the SuDS captured 14,770 measurements of storm drain water levels and 38,616 images. There were four data gaps in storm drain water levels during the study period due to battery depletion in the pressure logger (8/14 - 8/19, 9/20 - 9/22, 10/14 - 10/15, 10/25 - 11/04), totaling 21 days of missing data (13% of study period). Based on camera images, two roadway flood events occurred during these data gaps (10/29 and 11/4); however, because we do not have in situ knowledge of stormwater capacity from the pressure loggers, we do not include these floods in our calculation of flood frequency or discussion of flood drivers below.

On every day of measurement, the SuDS pressure logger recorded water from the tidal creek (receiving water body) entering the storm drain with each rising tide. Hence, the stormwater network was always at reduced drainage capacity at high tide, meaning that the network of pipes and catch basins could not convey runoff from the roadway to the tidal creek as designed during a rain event. We identified 24 discrete flood events where water levels surpassed the elevation of the top of the storm drain and then receded back into the drain. Using this definition of a flood event, it is possible to have more than one event in a day. However, given this definition, not all of the detected floods extended onto the roadway and impacted roadway functioning. As illustrated by the roadway cross-section in Figure 4, flood extent during 11 flood events was limited to parking spaces, 6 extended into the roadway, and an additional 7 flood events overtopped the curb and extended onto the sidewalk. Notably, 20 of the 24 floods were below the NOAA Beaufort high tide flood threshold (0.54 meters MHHW or 3.34 feet NAVD88, Sweet et al., 2020), 9 of which extended into the roadway.

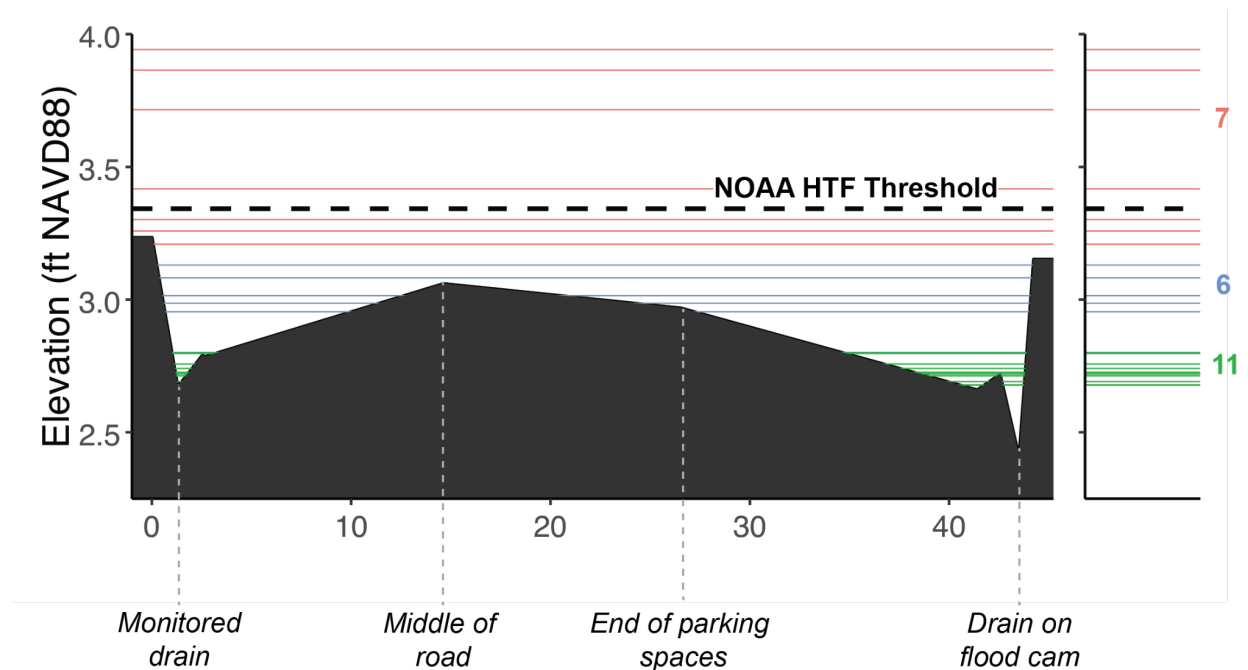


**Figure 4.** Cross section of the roadway and measured flood events by the SuDS pressure logger in Beaufort, NC between June 22 and November 30, 2021. Here we define a flood event as water levels surpassing the elevation of the top of the storm drain. Water levels above the monitored drain are interpolated across the roadway, but the spatial extent was also confirmed using camera images (e.g., Figures 5 and 6).

The 24 measured flood events in Beaufort can be classified into two types based on drivers, which we identify using imagery, the shape of the stormwater hydrograph, and local precipitation data. The first type of flooding – “sunny-day flooding” – is caused by high water levels in the tidal creek which fill the stormwater network until water overtops onto the street (Figure 5A). The shape of the storm drain hydrographs for these floods are smooth and periodic, following the predicted tide (Figure 5B). The second type of flooding – “rainy-day flooding” – occurs during rain storms, wherein elevated water levels in the tidal creek reduce the capacity of

the stormwater network such that runoff floods the roadway (Figure 6A). The storm drain hydrographs for this type of flooding are characterized by sharp increases in water level above the longer period fluctuations, which coincide with rain events (Figure 6B-C). We do not classify these floods further based on tidal influence primarily because we found that rainy-day floods occurred at all stages of the tide (rising, peak, and ebbing). It is also unclear to what extent high groundwater contributes to flood occurrence or extent.

Using these definitions, we observed 18 sunny-day and 6 rainy-day flood events over the 5 month study. The two types of flood events had distinctly different flood durations and magnitudes (Figure 7A). Sunny-day flood events were long in duration (median duration = 86.6 min) and led to the highest magnitude of flooding during the study period (1.27 feet above the top of the storm drain). Rainy-day flooding was much shorter in duration than sunny-day flooding (median duration = 10.9 min), and spanned a smaller range of flood magnitudes (0.1-0.6 feet above the top of the storm drain).

A)



B)

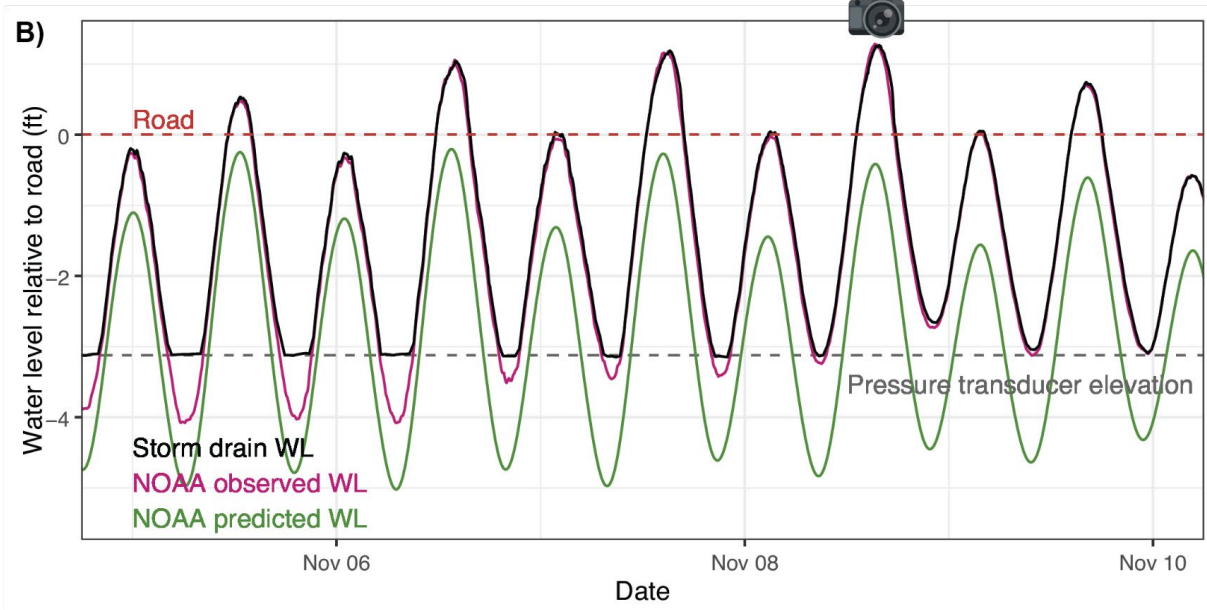


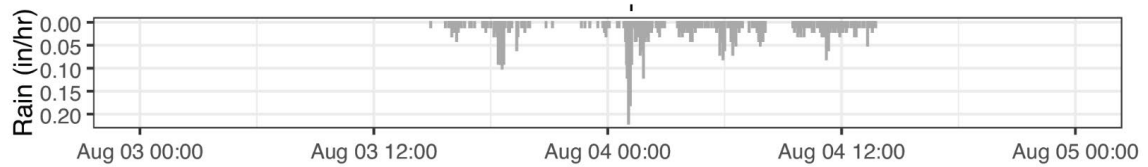
**Figure 5.** A series of “sunny-day” flood events measured in November 2021 in Beaufort, NC. **A)** Photo of the flooded roadway during the highest observed water level on November 8, 2021, and **B)** measured water levels above the storm drain pressure transducer relative to the road surface.



A)



B)



C)

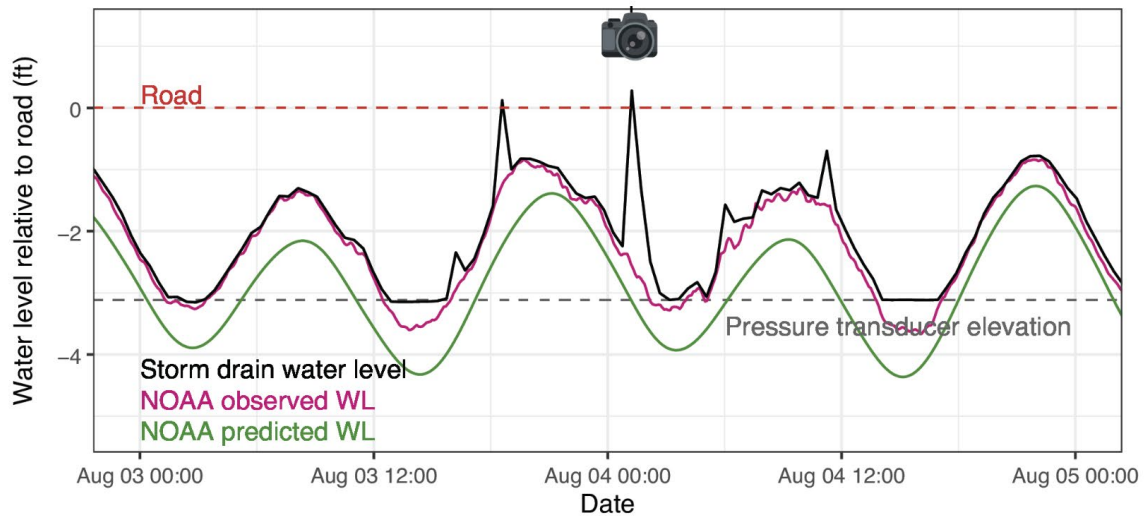


**Figure 6.** Two “rainy-day” flood events on August 3 and 4, 2021 in Beaufort, NC. **A)** Photo of the flooded roadway during the August 3 flood event, **B)** 5-min rain intensity from the Beaufort Smith Field precipitation gauge (see Figure 3A), and **C)** measured water levels above the storm drain pressure transducer relative to the road surface.

### 3.2 Comparison with tide gauge-based flood thresholds

Storm drain water levels during sunny-day flood events showed a strong agreement with NOAA tide gauge water level observations (RMSE=0.1 ft), whereas measured water levels during rainy-day floods diverged greatly from tide gauge observations (RMSE = 1.81 ft). The NOAA HTF flood threshold for the Beaufort tide gauge is 3.34 ft NAVD88, which spans just above the crest of the roadway at the location of the SuDS (Figure 4). Of the 20 floods that we measured below the NOAA HTF flood threshold, 6 were rainy-day floods. Hence, while this tide gauge-based proxy captures roadway flood contributions from high water levels in Taylors Creek, it misses the rainy-day events that occur due to a combination of land-based factors: here, rainfall runoff and reduced capacity in stormwater infrastructure. Although the data in this study only span 5 months, the rainy-day events constitute 25% of all floods. This finding suggests that tide-gauge proxies likely underestimate flood frequency in areas where the stormwater network is still at full or partial capacity.

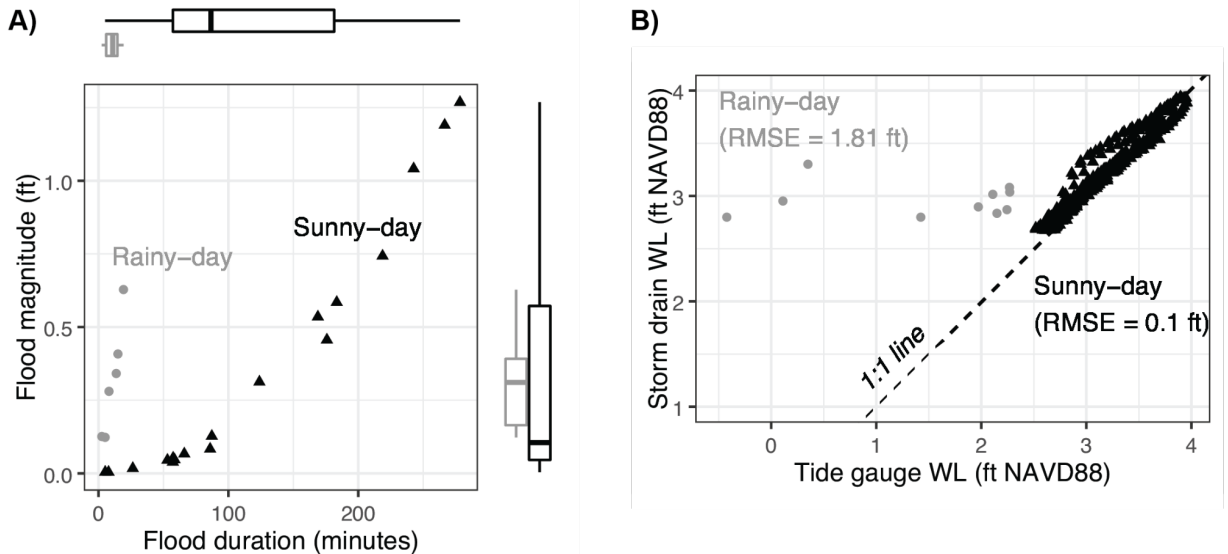


**Figure 7.** **A)** Comparison of flood magnitude (i.e., depth of water above the top of the storm drain) and duration for both sunny-day and rainy-day floods, with boxplots showing the distribution of each variable for all floods. **B)** Comparison of measured storm drain water levels during sunny-day and rainy-day floods to water levels recorded at the local NOAA tide gauge.

### 3.3 Sensor limitations

The SuDS have supplied a rare look at conditions within storm drains prior to chronic floods in Beaufort, NC. As a low-cost sensor framework, however, there are limitations. First, we found that the low-cost pressure transducer is sensitive to temperature, despite on-board manufacturer supplied corrections, and needs to be calibrated prior to use to ensure data quality. Second, we have documented (and corrected for) drift in the pressure measurements that may be caused by prolonged inundation or intermittent wetting-drying cycles (Figure S1). A more robust pressure transducer would likely eliminate these limitations, albeit at an increase to the sensor cost. Third, the SuDS framework uses Bluetooth to send data from the pressure logger to the gateway, but the range of this connection is impeded by the metal grate covering the storm drain.



This means the gateway and pressure logger must be fairly close to each other (line of sight) for consistent data uploads. Lower bandwidth communications technologies (i.e., LoRa) could be used to extend the distance between the monitored storm drain and gateway. Finally, the SuDS provide real-time data at all times except when the logger is inundated and unable to transfer data to the gateway. This loss of communications is a common drawback of flood-sensing technologies that rely on wireless communication. But contrary to other technologies, our logger continues to collect water level data while underwater and transfers the data once communications are re-established. The roadway camera within the gateway also provides near real-time pictures of the roadway even when water level sensor communications are interrupted.

### 3.4 Implications for community engagement and hazard communication

The SuDS sensor framework presented here can contribute to enhanced flood awareness and public safety in the near-term, as well as improved resilience to climate change in the long-term. Local officials typically block off flooded roads to protect public safety, but with chronic flooding, it is not always evident when roads will need to be closed and when they can be reopened. The SuDS framework can be used to notify emergency management officials when water levels begin to approach the roadway or once water levels have receded. Such alerts reduce the risk of vehicle damage and minimize the duration of disruptions, as the road can be reopened promptly. Local residents can also view images in real-time on the web app to determine if they can travel safely or need to adjust their plans (“Flood Cam” tab in Figure 8).

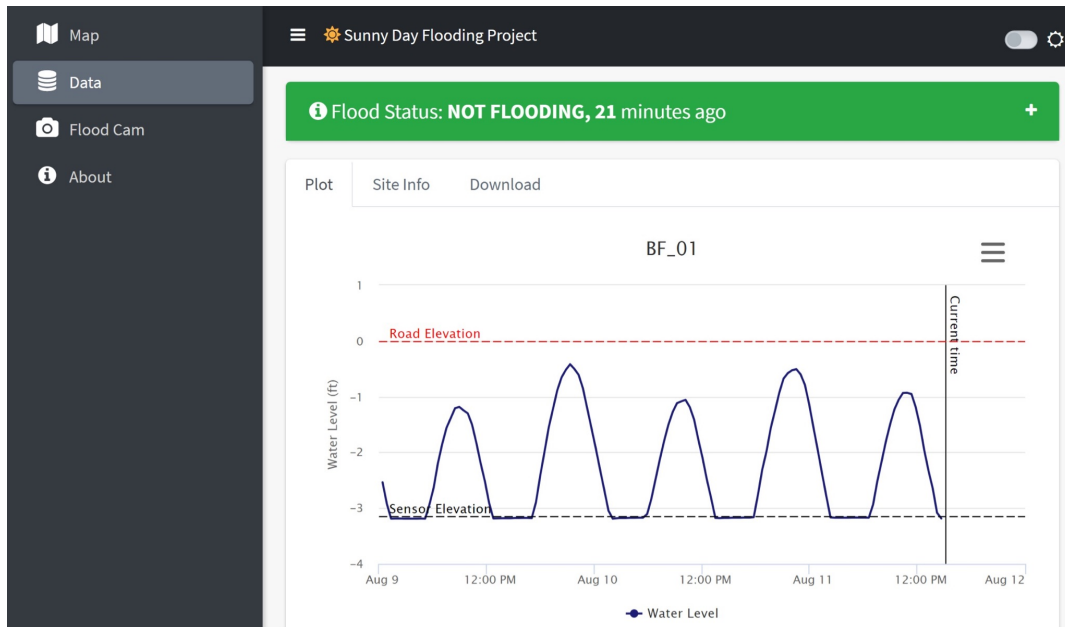


**Figure 8.** Screenshot of the SuDS web app showing live water level data from the monitored storm drain in Beaufort, NC. This web app also shows sample sites (and flooding status) on an overview map (“Map” tab), real-time images from SuDS gateway cameras (“Flood Cam” tab), and information about the project (“About” tab).

The SuDS framework can be used to support broader public engagement and education efforts concerning the impacts of climate change. Unlike many climate impacts, chronic coastal

flooding is visible, frequent, and can be directly linked to SLR. For example, the SuDS framework could be integrated into a community science project to document the extent and disruptions associated with tidal floods (e.g., King Tides Project, n.d.). Informational signs near the SuDS can raise awareness around the issue of chronic flooding and the impacts of SLR.

As communities increasingly prepare for higher sea levels, a stronger understanding of the incidence and drivers of chronic flooding can inform evidence-based adaptation plans and investments. First, data from the SuDS framework can help identify the relative contributions of rainfall and high-water levels in receiving water bodies. Such evidence is valuable because some adaptation strategies may only combat flooding from one source. For example, higher bulkheads can prevent overtopping, but will not prevent water from entering through the stormwater network. Second, the SuDS framework can improve estimates of future flood frequency by identifying the range of conditions that lead to flooding. Adaptation strategies designed for extreme events, such as high sand dunes, will have little effect or exacerbate smaller floods along the back-side of islands or bays. With greater evidence on how chronic flooding will evolve into the future, communities can assess their needs and priorities and allocate resources accordingly.

Finally, the SuDS framework is purposefully open-source and low-cost, with the goal of enabling broader adoption by researchers and community members alike. Chronic coastal flooding is ubiquitous in low-lying coastal communities, and many questions remain about its drivers and impacts. By monitoring flooding where people live and by capturing flooding from multiple drivers, this sensor framework can enable widespread progress in understanding the causes of such events and devising potential solutions.

## Open Research

The storm drain water level data used for flood detection and analysis in the study are available for download on our project web app (<https://sunnydayflood.apps.cloudapps.unc.edu>). Prior to peer-reviewed publication, these data will be archived on Zenodo with their own DOI. The software for the SuDS sensor framework are available on GitHub (<https://github.com/sunny-day-flooding-project>), and prior to peer-reviewed publication, the referenced repositories will be archived with Zenodo and assigned a DOI for the most current release.

## References

- Befus, K. M., Barnard, P. L., Hoover, D. J., Finzi Hart, J. A., & Voss, C. I. (2020). Increasing threat of coastal groundwater hazards from sea-level rise in California. *Nature Climate Change*, *10*(10), 946–952. <https://doi.org/10.1038/s41558-020-0874-1>
- Bernstein, A., Gustafson, M. T., & Lewis, R. (2019). Disaster on the horizon: The price effect of sea level rise. *Journal of Financial Economics*, *134*(2), 253–272. <https://doi.org/10.1016/J.JFINECO.2019.03.013>
- Bronen, R., & Chapin, F. S. (2013). Adaptive governance and institutional strategies for climate-induced community relocations in Alaska. *Proceedings of the National Academy of Sciences of the United States of America*, *110*(23), 9320–9325. <https://doi.org/10.1073/PNAS.1210508110>
- Coutu, P. (2021, January 3). In Norfolk, sea level rise reduces some stormwater system capacity by 50%, data shows. *The Virginian-Pilot*. Retrieved from <https://www.pilotonline.com/news/environment/vp-nw-fz20-sensor-stormwater-flooding->

- norfolk-20210103-t4jofv7hbff3dgcposbf7z7p5m-story.html
- Dahl, K. A., Fitzpatrick, M. F., & Spanger-Siegfried, E. (2017). Sea level rise drives increased tidal flooding frequency at tide gauges along the U.S. East and Gulf Coasts: Projections for 2030 and 2045. *PLoS ONE*, *12*(2), 1–23. <https://doi.org/10.1371/journal.pone.0170949>
- FloodNet. (2022). FloodSense Sensor Technical Documentation. Retrieved from <https://github.com/floodnet-nyc/flood-sensor>
- Gold, A. C., Brown, C. M., Thompson, S. P., & Piehler, M. F. (2022). Inundation of Stormwater Infrastructure is Common and Increases Risk of Flooding in Coastal Urban Areas along the US Atlantic Coast. *Earth's Future*. <https://doi.org/10.1029/2021EF002139>
- Gold, A. C., Anarde, K., Grimley, L., Neve, R., Srebnik, E. R., Thelen, T., et al. (2022). Sunny Day Flooding Project Tutorials. Retrieved from <https://github.com/sunny-day-flooding-project/tutorials>
- Gornitz, V., Oppenheimer, M., Kopp, R., Horton, R., Orton, P., Rosenzweig, C., et al. (2020). Enhancing New York City's resilience to sea level rise and increased coastal flooding. *Urban Climate*, *33*, 100654. <https://doi.org/10.1016/J.UCLIM.2020.100654>
- Habel, S., Fletcher, C. H., Anderson, T. R., & Thompson, P. R. (2020). Sea-Level Rise Induced Multi-Mechanism Flooding and Contribution to Urban Infrastructure Failure. *Scientific Reports*, *10*(1), 1–12. <https://doi.org/10.1038/s41598-020-60762-4>
- Hauer, M. E., Evans, J. M., & Mishra, D. R. (2016). Millions projected to be at risk from sea-level rise in the continental United States. *Nature Climate Change*, *6*(7), 691–695. <https://doi.org/10.1038/nclimate2961>
- Jane, R., Cadavid, L., Obeysekera, J., & Wahl, T. (2020). Multivariate statistical modelling of the drivers of compound flood events in south Florida. *Natural Hazards and Earth System Sciences*, *20*(10), 2681–2699. <https://doi.org/10.5194/NHESS-20-2681-2020>
- King Tides Project. (n.d.). King Tides Project. Retrieved March 17, 2022, from <https://kingtides.net>
- Loftis, D., Forrest, D., Katragadda, S., Spencer, K., Organski, T., Nguyen, C., & Rhee, S. (2018). StormSense: A New Integrated Network of IoT Water Level Sensors in the Smart Cities of Hampton Roads, VA. *Mar Technol Soc J*, *52*. <https://doi.org/10.4031/MTSJ.52.2.7>
- Lyman, T. P., Elsmore, K., Gaylord, B., Byrnes, J. E. K., & Miller, L. P. (2020). Open Wave Height Logger: An open source pressure sensor data logger for wave measurement. *Limnology and Oceanography: Methods*, *18*(7), 335–345. <https://doi.org/10.1002/lom3.10370>
- Maisano, L., Cuadrado, D. G., & Gómez, E. A. (2019). Processes of MISS-formation in a modern siliciclastic tidal flat, Patagonia (Argentina). *Sedimentary Geology*, *381*, 1–12. <https://doi.org/10.1016/j.sedgeo.2018.12.002>
- Merkel, D. (2014). Docker: lightweight Linux containers for consistent development and deployment. *Linux Journal*. Retrieved from <http://www.docker.io>
- Moftakhari, H. R., AghaKouchak, A., Sanders, B. F., & Matthew, R. A. (2017). Cumulative hazard: The case of nuisance flooding. *Earth's Future*, *5*(2), 214–223. <https://doi.org/10.1002/2016EF000494>
- Molinarioli, E., Guerzoni, S., & Suman, D. (2019). Do the Adaptations of Venice and Miami to Sea Level Rise Offer Lessons for Other Vulnerable Coastal Cities? *Environmental Management*, *64*(4), 391–415. <https://doi.org/10.1007/S00267-019-01198-Z/TABLES/3>
- Moore, F. C., & Obradovich, N. (2020). Using remarkability to define coastal flooding thresholds. *Nature Communications* *2020 11:1*, *11*(1), 1–8. <https://doi.org/10.1038/s41467->

019-13935-3

- Sweet, W., Dusek, G., Carbin, G., Marra, J., Marcy, D., & Simon, S. (2020). *2019 State of U.S. High Tide Flooding with a 2020 Outlook* (Vol. NOAA Techn). Retrieved from [https://www.ncdc.noaa.gov/monitoring-content/sotc/national/2017/may/2016\\_StateofHighTideFlooding.pdf](https://www.ncdc.noaa.gov/monitoring-content/sotc/national/2017/may/2016_StateofHighTideFlooding.pdf)
- Sweet, W. V., Dusek, G., Obeysekera, J., & Marra, J. J. (2018). Patterns and projections of high tide flooding along the U.S. coastline using a common impact threshold. *NOAA Technical Report NOS CO-OPS 086*, (February).
- Temple, N. A., Webb, B. M., Sparks, E. L., & Linhoss, A. C. (2020). Low-Cost Pressure Gauges for Measuring Water Waves. *Journal of Coastal Research*, *36*(3), 661. <https://doi.org/10.2112/JCOASTRES-D-19-00118.1>
- Ware, M., & Fuentes, M. M. P. B. (2018). A comparison of methods used to monitor groundwater inundation of sea turtle nests. *Journal of Experimental Marine Biology and Ecology*, *503*, 1–7. <https://doi.org/10.1016/j.jembe.2018.02.001>

Supporting Information for

**Data from the drain: a sensor framework that captures multiple drivers of chronic floods**

**Adam Gold<sup>1</sup>, Katherine Anarde<sup>2</sup>, Lauren Grimley<sup>3</sup>, Ryan Neve<sup>4</sup>, Emma Rudy Srebnik<sup>5</sup>, Thomas Thelen<sup>2</sup>, Anthony Whipple<sup>4</sup>, Miyuki Hino<sup>5,6</sup>**

<sup>1</sup>University of North Carolina at Chapel Hill Institute for the Environment, Chapel Hill, NC

<sup>2</sup>North Carolina State University, Department of Civil, Construction, and Environmental Engineering, Raleigh, NC

<sup>3</sup>University of North Carolina at Chapel Hill, Department of Earth, Marine and Environmental Sciences, Chapel Hill, NC

<sup>4</sup>University of North Carolina at Chapel Hill Institute of Marine Sciences, Morehead City, NC

<sup>5</sup>University of North Carolina at Chapel Hill, Environment, Ecology, and Energy program, Chapel Hill, NC

<sup>6</sup>University of North Carolina at Chapel Hill, Department of City and Regional Planning and Environment, Chapel Hill, NC

**Contents of this file**

Figure S1

## Introduction

Drift detection and correction is performed using atmospherically-corrected pressure data converted to water depth. First, a rolling function that calculates the minimum water depth over the past two days is applied to uncorrected water depth data. These rolling minimum water depth values are fit with a loess function to smooth the data and account for any short-term variations, such as if the logger is inundated for multiple days. Second, to correct for drift, an offset is applied to the uncorrected water depth data, and this offset is the difference between the surveyed sensor elevation and the smoothed minimum water depth.

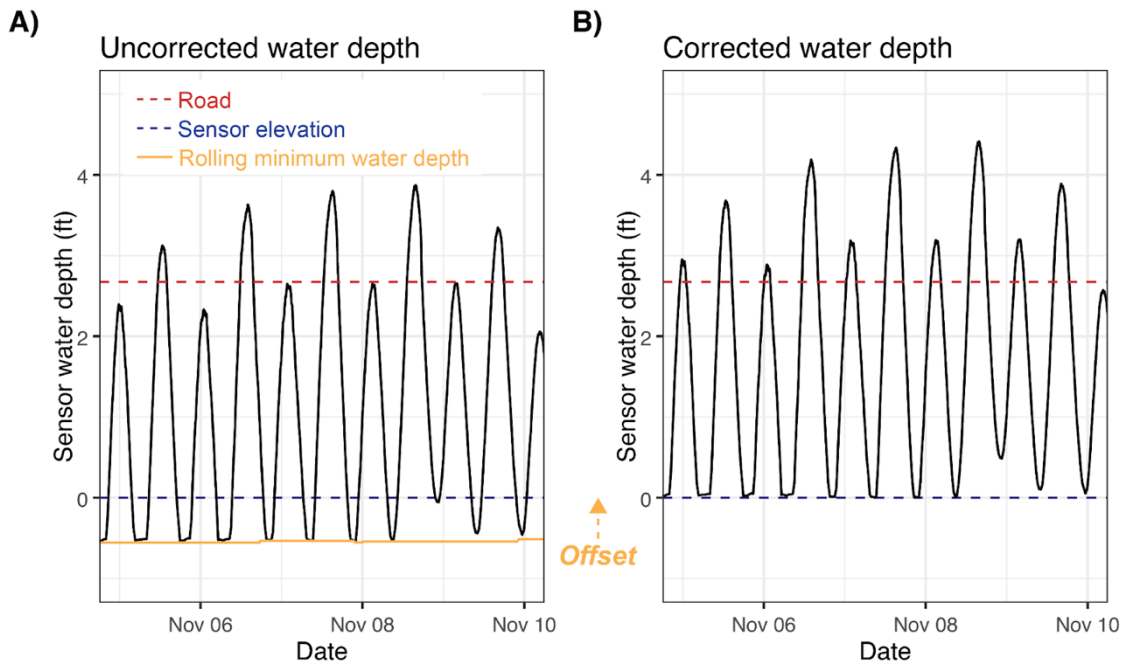


**Figure S1.** Graphical explanation of pressure sensor drift detection (A) and correction (B).